[Tectonics]

Supporting Information for

Lithospheric Strength and Rift Migration controls on Syn-rift Stratigraphy and Breakup Unconformities at Rifted Margins: Examples from Numerical Models, the Atlantic and South China Sea Margins

M. Pérez-Gussinyé[1], M. Andrés-Martínez[1], M. Araujo[1,2], Y. Xin[1,3], J. Armitage[4], J. P. Morgan[5]

[1]MARUM-Center for Marine Environmental Sciences, University of Bremen, Bremen, Germany

[2] CENPES Research Center, Petrobras, Brazil.

[3]Guangzhou Institute of Geochemistry, Guangzhou, Chinese Academy of Science, China.

[4]IFP Energies Nouvelles, Rueil-Malmaison, France

[5]Department of Ocean Science and Engineering, SUSTech, Shenzen, China.

Contents of this file

Additional Supporting Information (Files uploaded separately)

Introduction

The supporting information contains 10 figures, A1 to A10, two Table S1 and 9 movies, Movie_S1 to Movie_S9.

Random weak seed implementation

Geodynamic numerical models need of weak seeds to localize deformation in the center of the model domain at the beginning of the run, otherwise deformation would typically localize in the lateral boundaries. Weak seeds such as an increase of temperature (TWS) or a low viscosity seed, tend to strongly localize deformation at the initial phases of rifting, partly inhibiting initial phases of distributed extension observed in many natural examples. The Random weak seed WS is designed to allow initial distributed deformation while avoiding the deformation to go to the lateral boundaries. In the following sections we explain the strain softening functions used in the experiments and how the random damage seed modifies the strain softening input parameters to generate a random distributed damage.

Strain softening

As parameters for the strain softening we have an initial and final values of the friction angle (θ_0 and θ_1) and corresponding strains for these values (E_0 and E_1). These parameters define the slope of the strain softening function ($\frac{\theta_1-\theta_0}{E_1-E_0}$):

$$\theta = \frac{\theta_1-\theta_0}{E_1-E_0} E + \theta_0$$

where E is the second invariant of the strain an θ is the calculated friction angle used for solving plasticity. In the experiments θ_0 is generally defined as 30 and θ_1 as 15, while the corresponding strains (E_0 and E_1) are 0 and 1. The equivalent formula is used in the calculation of the viscous softening, where the preexponential factor is multiplied by 1 when the strain is 0 and by 30 when the strain reaches 1.

Random damage week seed

The random weak seed used in this work for some of the numerical experiments, consist of a distributed random damage, both in the plastic and viscous fields. At the beginning of the model, a random field is calculated for all the integration points with values between 0 and 1. This random field is treated as a material property and, therefore, advected every time step.

Then, this random damage field is multiplied by a given amplitude of variation of the initial friction angle. For the experiments presented here this variation of the friction angle is of a maximum of 4 degrees, meaning that the initial friction angle across the model domain takes random values in the range of 26 and 30 degrees. The lower bound of this range diminishes gradually, following a horizontal-space Gaussian function of 200 km wave length (Figures A3c–d). Outside of the weak seed region the lower bound has values of 29 degrees, while in the center the weak seed it reaches a minimum of 26 degrees (i.e. the initial friction angle at the integration points in the center of the model can take values between 26 and 30 degrees, see

Figure A3c). Also, E_1 is modified according to the random field to preserve the strain softening slope ($\frac{\theta_1-\theta_0}{E_1-E_0}$) across the model domain (Figure A3a). This physically means that strain softening occurs at the same rate across the model domain, and can be thought as if the integration points with initial friction angle smaller than 30 have undergone some random deformation previous to the model run (i.e. random damage, see Figure A3a). The same occurs for the initial viscous preexponential softening factor (PEF0), whose initial value at the center of the weak seed can be in the range of 1 to 6 (Figure A3b). Note that the calculation of the lower bound of those ranges using the Gaussian function is done at the beginning of the experiment and advected with the material, so that initial random damage and the softening functions are material properties.

Hemipelagic sedimentation in the sea

Hemipelagic sediments are added to the landscape evolution model as a source term on the sea:

$$\frac{\partial h}{\partial t} = \frac{\partial}{\partial x}\left(K_s e^{(-\lambda_s h_w)} \frac{\partial h}{\partial x}\right) + S$$

where *h* is the topography, *t* is the time, *x* the horizontal distance, K_s is the submarine diffusion coefficient, λ_s is the submarine diffusion decay coefficient, h_w is the water depth (the difference between sea level and the submarine topography), and *S* is the hemipelagic source term.

Figures

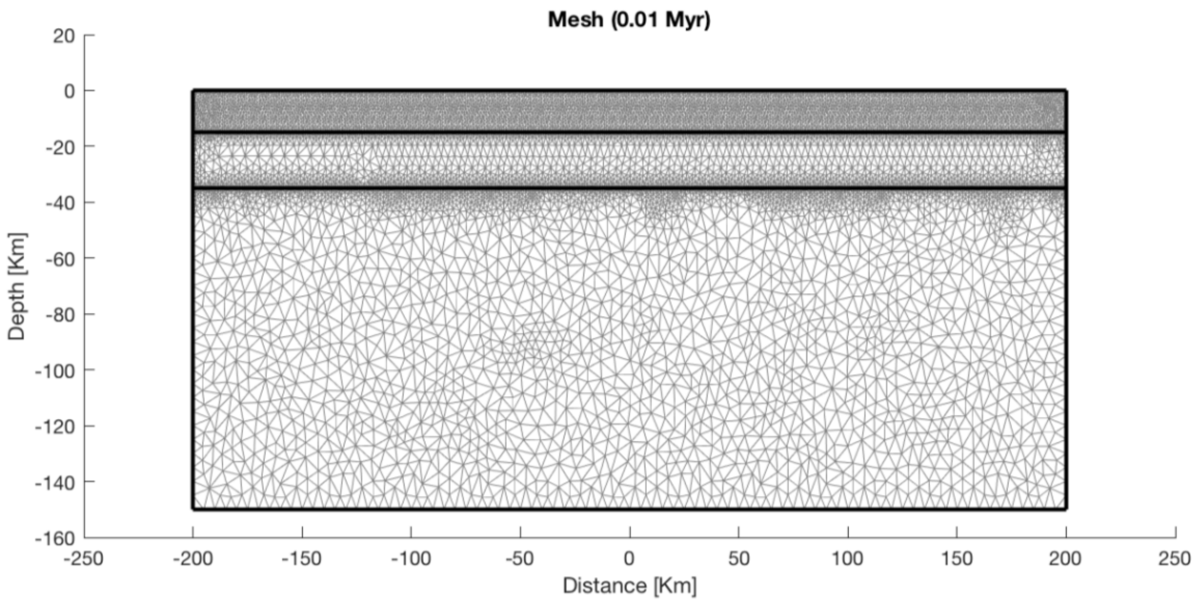

Figure S1. Initial mesh configuration, showing the initial grid consisting of an upper crustal layer UC, a lower crustal layer, LC and the mantle layer consisting of lithosphere and asthenosphere. The rheological parameters for the UC, LC and mantle are given in Table 2. Table 1 describes the different models generated in this work by changing lower crustal rheology, crustal thickness, geotherm and initialization of deformation.

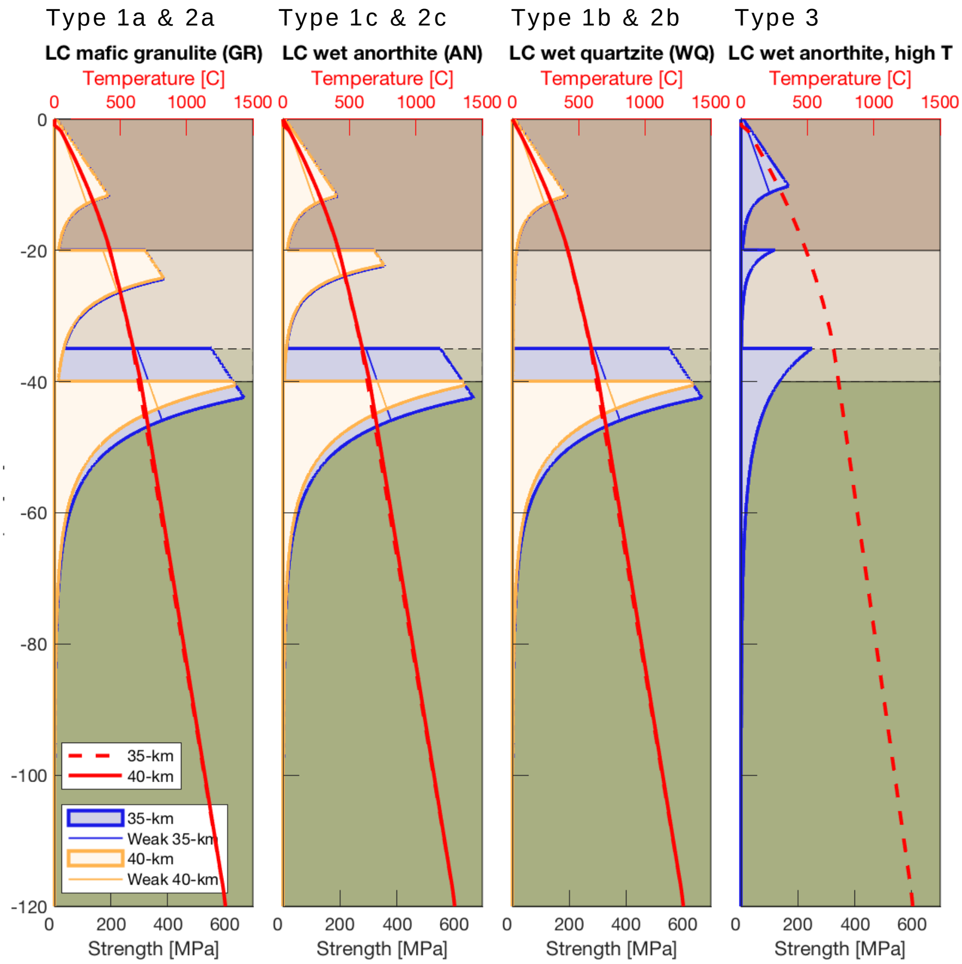

Figure S2. Initial strength and temperature profiles, away from the initial weak seed, for the models shown in this work (see Table 1). Lower crustal rheologies used are mafic granulite, GR, wet anorthite, AN, and wet quartzite, WQ (see Table 2 for rheological parameters). The blue envelopes are for 35 km crust and the orange ones for 40 km thick crust. Red solid and dashed lines are the geotherm in each case. The first 3 columns correspond to a model initialized with a thermal weak seed, TWS, at the model center and a geotherm with 600 ºC at 35 km (Types 1a-c, 2a-c). The fourth column corresponds to a model initialized with a random weak seed, anorthite in the lower crust, a 35 km crust and a temperature of 700 ºC at 35 km (Type 3). Figure 1 shows the final architectures of some of these models. The strength profiles do not show the effect of the initial weak seed. They are computed with a strain rate of 10^{-15} s^{-1}. The effect of the initial weak seed on viscosity is shown in Figure A4.

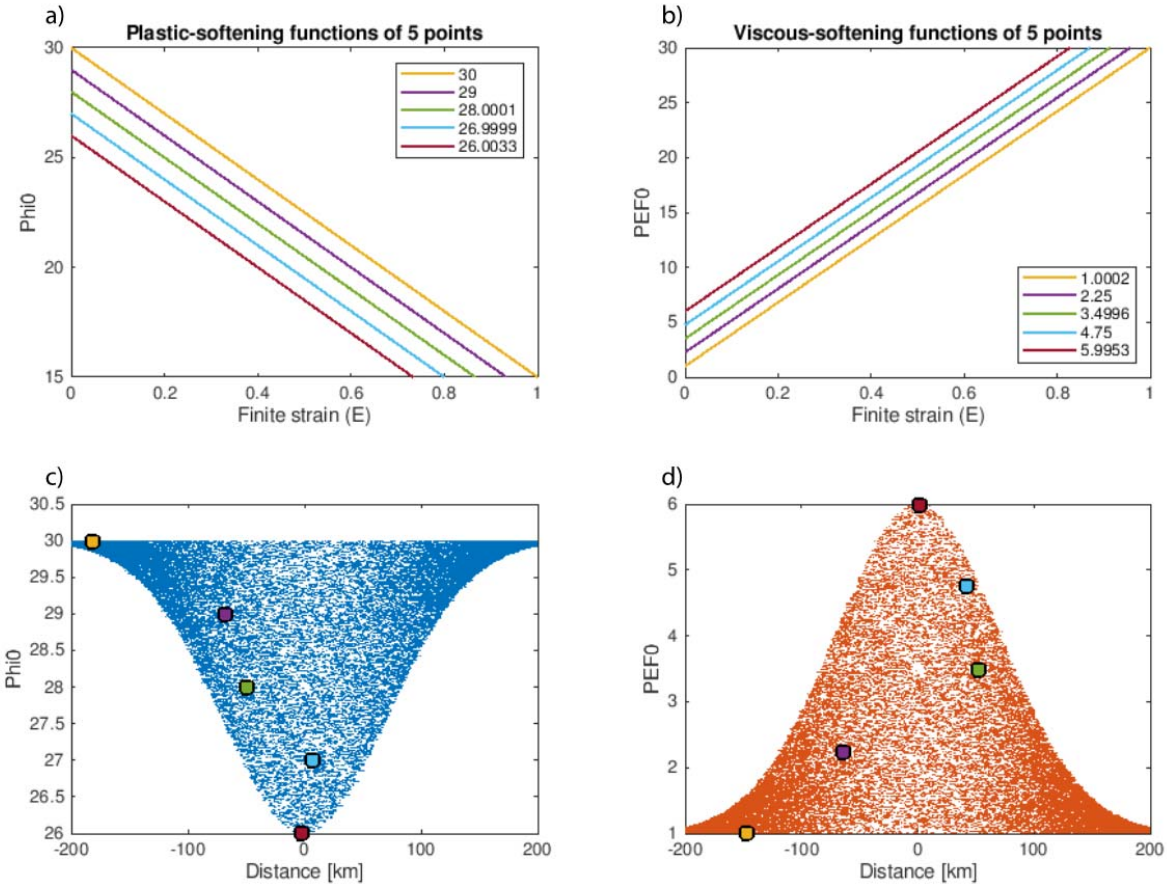

Figure S3. Plastic and viscous strain softening functions with random weak seeds shown for the first time step. (a) Plastic strain softening of 5 integrations points. The yellow line represents a case of no damage as the initial friction angle is 30. The other points are randomly damaged (initial friction angles between 15 and 30) and therefore, their strain softening functions have an offset (purple, green, cyan and crimson lines). (b) Viscous strain softening of 5 integrations points. The yellow line represents a case of no damage as the initial preexponential multiplier is 1. The other points are randomly damaged (initial preexponential multiplier between 1 and 6) and therefore, their strain softening functions have an offset (purple, green, cyan and crimson lines). (c) Initial friction angle at all integration points plotted against distance along the model section. Note how the minimum initial friction angle follows a Gaussian function reaching a minimum of 26. The large points correspond to the lines of the same color in (a). (d) Initial preexponential multiplier at all integration points plotted against distance along the model section. Note how the minimum initial preexponential multiplier follows a Gaussian function reaching a maximum of 6. The large points correspond to the lines of the same color in (b).

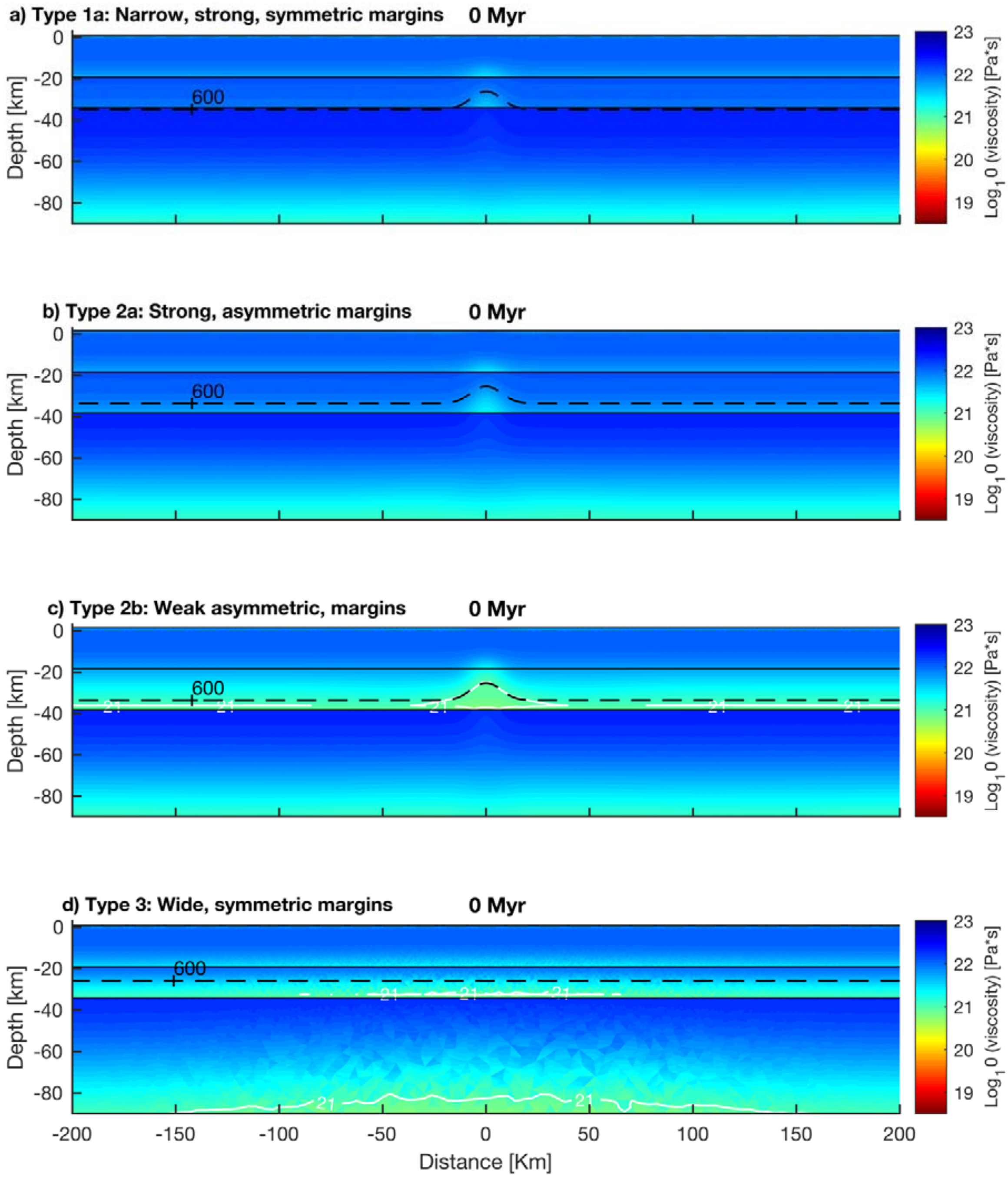

Figure S4. Initial viscosity profiles for the main 4 models shown in this work, corresponding to the strength profiles in Figure A2, and the models shown in Figure 1. TWS: initialization with thermal weak seed. RWS: initialization with a random weak seed. a) to c) are initialized with TWS and have a temperature of 600 ºC at 35 km at rift start. d) is initialized with RWS and has a temperature at 35 km of 700 ºC at rift start.

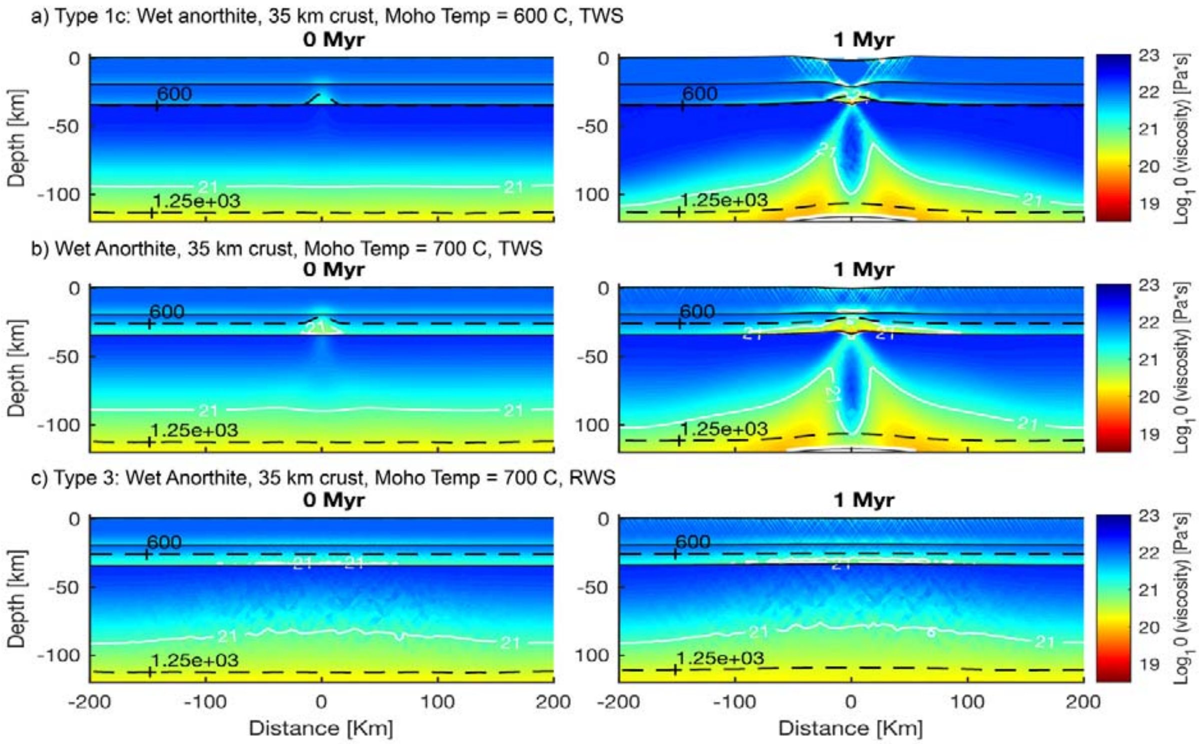

Figure S5. Viscosity profiles for wet anorthite lower crustal rheology, at 0 (left panel) and 1 (right panel) Myr after rift start, showing the effect on viscosity of an increase in Moho temperature and different weak seeds for initialization. TWS: initialization with thermal weak seed. RWS: initialization with a random weak seed. All models have a 35 km thick crust. a) Type 1c model (see Table 1) and b) are initialized with TWS and c) Type 3 model is initialized with RWS. a) has a temperature at the Moho of 600 ºC, b) and c) have a temperature at the Moho of 700 ºC, at rift start. These models result in different final configurations, see Figure A6.

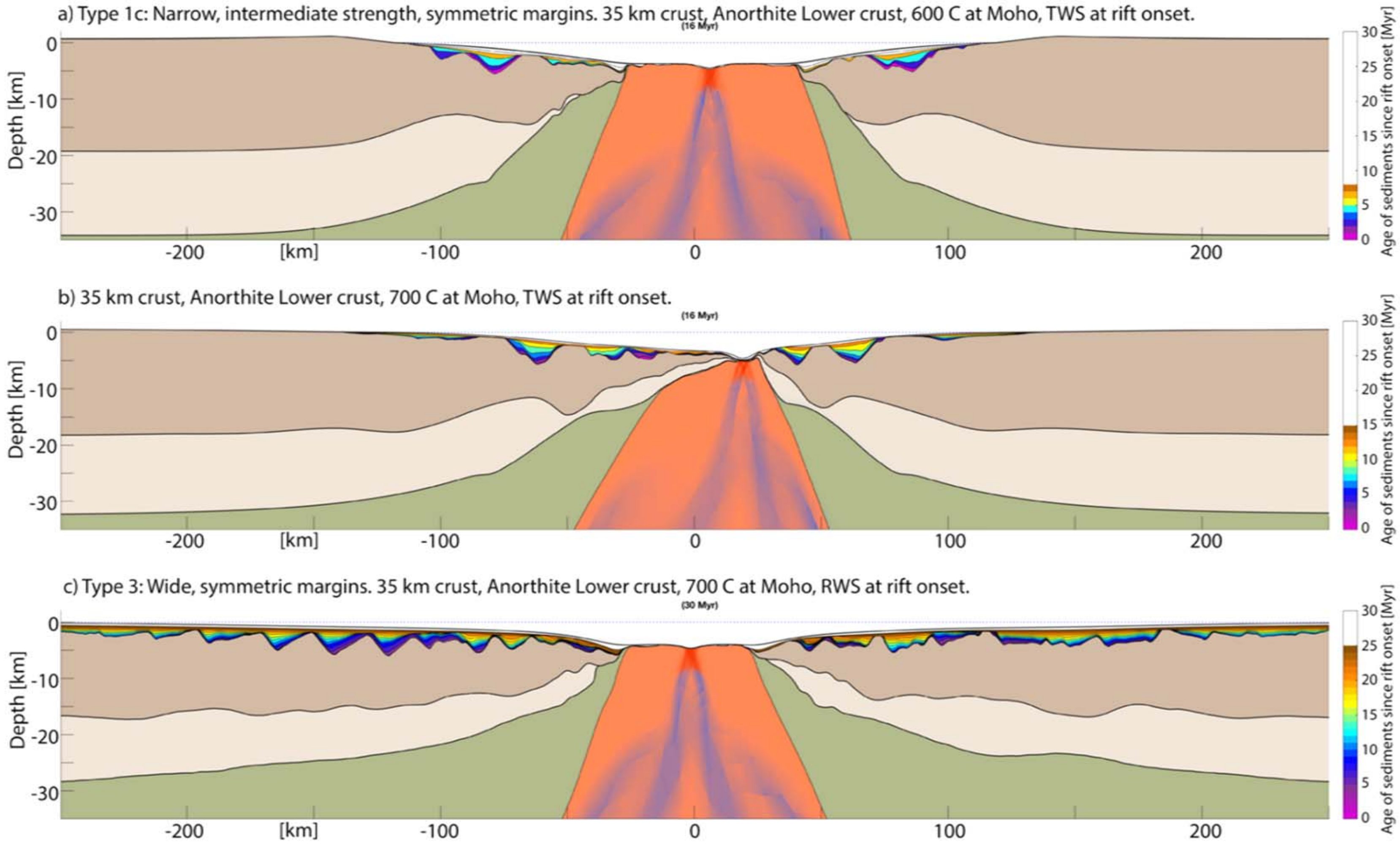
a) Type 1c: Narrow, intermediate strength, symmetric margins. 35 km crust, Anorthite Lower crust, 600 C at Moho, TWS at rift onset.
(16 Myr)
b) 35 km crust, Anorthite Lower crust, 700 C at Moho, TWS at rift onset.
(16 Myr)
c) Type 3: Wide, symmetric margins. 35 km crust, Anorthite Lower crust, 700 C at Moho, RWS at rift onset.
(30 Myr)
Depth [km]
0
-10
-20
-30
-200
[km]
-100
0
100
200
Age of sediments since rift onset [Myr]
30
25
20
15
10
5
0

Figure S6. Effect of increasing the initial geothermal gradient and changing the initial seed to focus the deformation at the start of rifting. The figure shows the geometry at breakup of the models shown in Figure A5. a) and b) are initialized with a thermal weak seed, TWS, and have a temperature of 600 ºC, and 700 ºC at Moho, respectively, at rift start. c) Has a temperature at Moho of 700 ºC, at rift start, and is initialized with a random weak seed, RWS. a) corresponds to Type 1c margins, and c) corresponds to Type 3 margins,

Figure S7. Snapshots of model evolution for Type 1a,b,c models. Model configuration is shown for a case where surface processes parameters are the same as in Figure 1a. Age of the sediment is shown in a rainbow color scale for the synrift and in white to red color scale for the postrift. Dashed blue line is the isostatically calculated sea-level, assuming a 30 km crust is at sea-level. Red and blue shades show plastic and ductile strain rate.

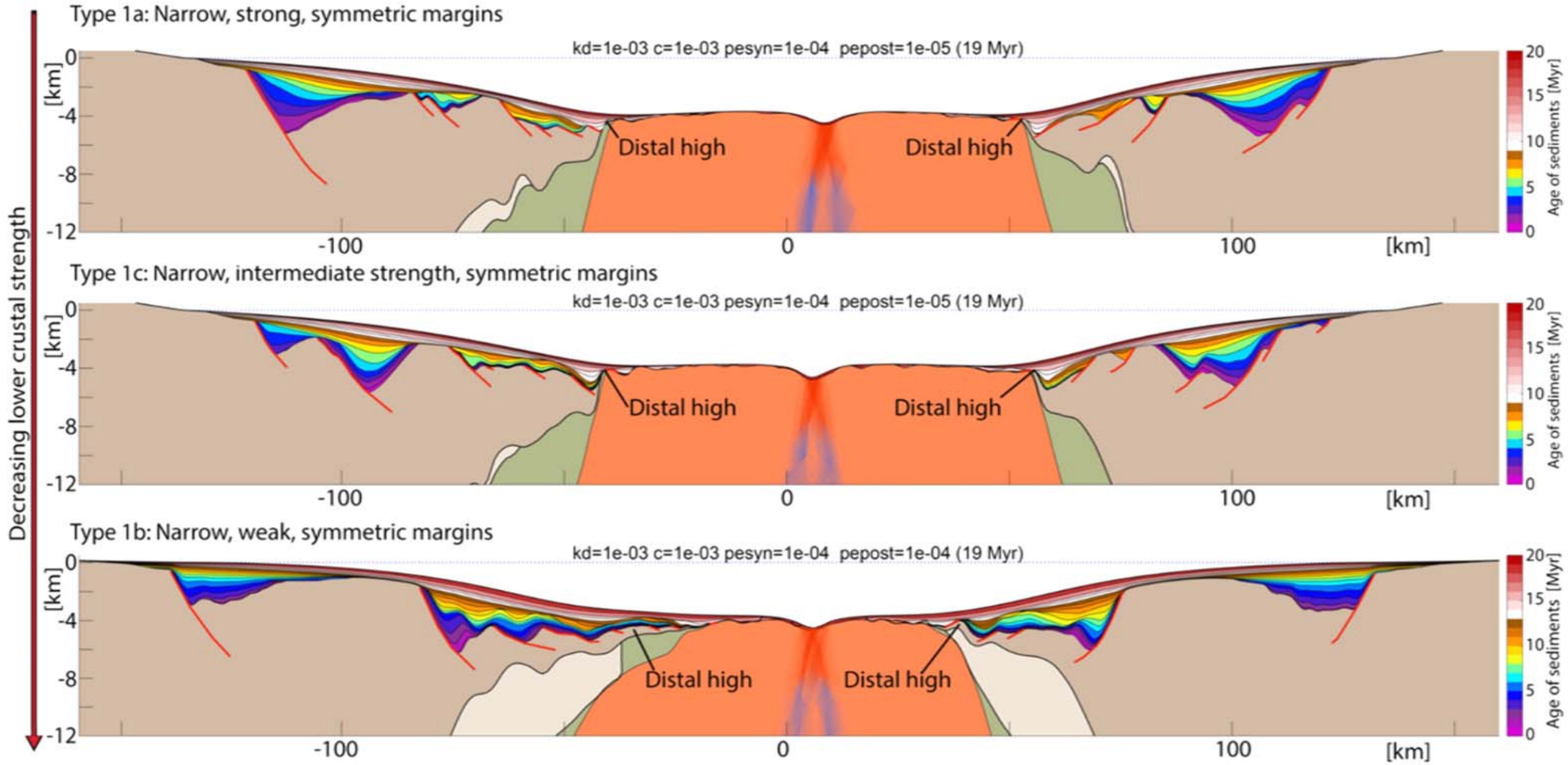

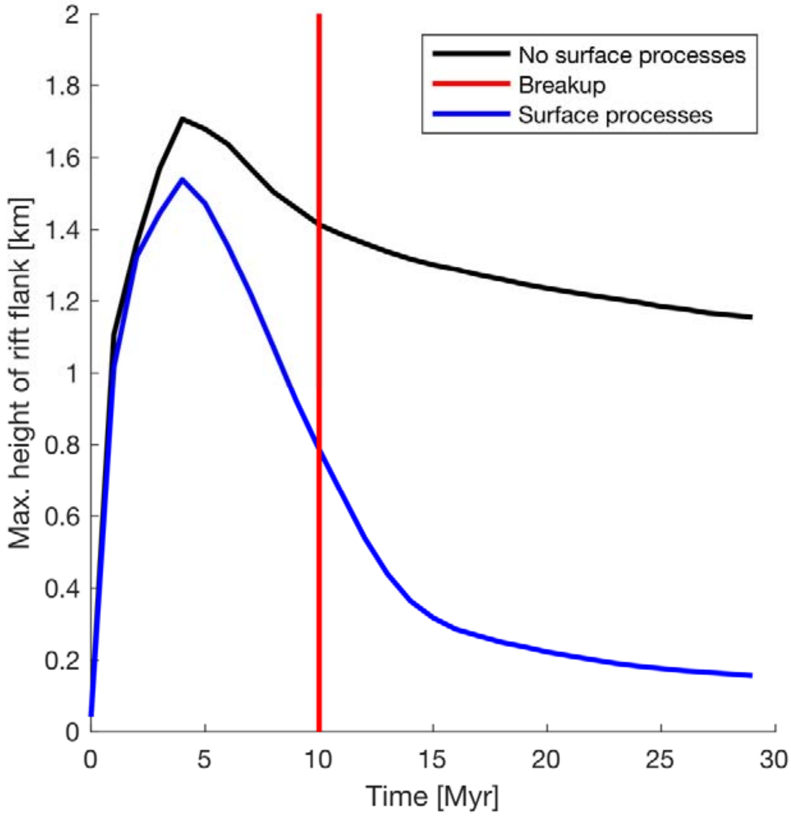

Figure S8. Evolution of the highest topographic point during model run, for Type 1a model (blue line, Figure 1a), and the same model without surface processes (black line). Note that the shoulder is at its highest position at around 4 Myr and then it gradually subsides as its bounding fault becomes abandoned and deformation migrates basinwards. In the model with surface processes, the shoulder is eroded, so its highest point is at lower elevations than in the model with no surface processes.

Figure S9. Effect of decreasing lower crustal strength in margin and sedimentary architecture, for a 40 km thick crust. Snapshots of model's evolution at 50 Myr and 60 Myr for Type 2a, b, and c margins (see Table 1). Top and bottom models are the same shown in Figures 4b and 6. The surface processes parameters in the case of wet anorthite, shown in the middle panel, are the same as in those models. Age of the sediment is shown in a rainbow color scale for the synrift and in white to red color scale for the postrift. Blue and red shadings are viscous and plastic strain rates, respectively. Dashed blue line is the isostatically calculated sea-level assuming that a 30 km crust is at sea-level.

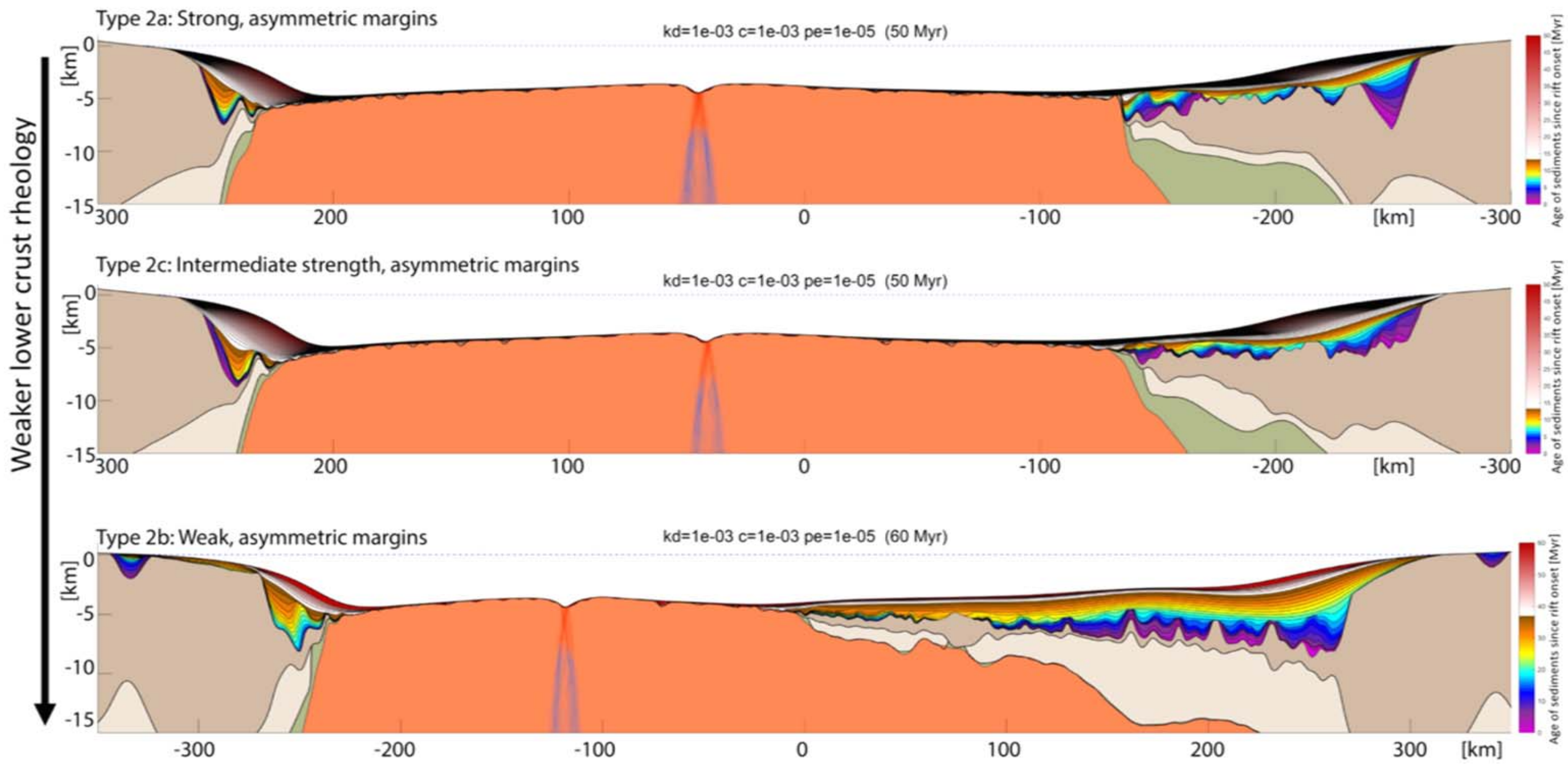

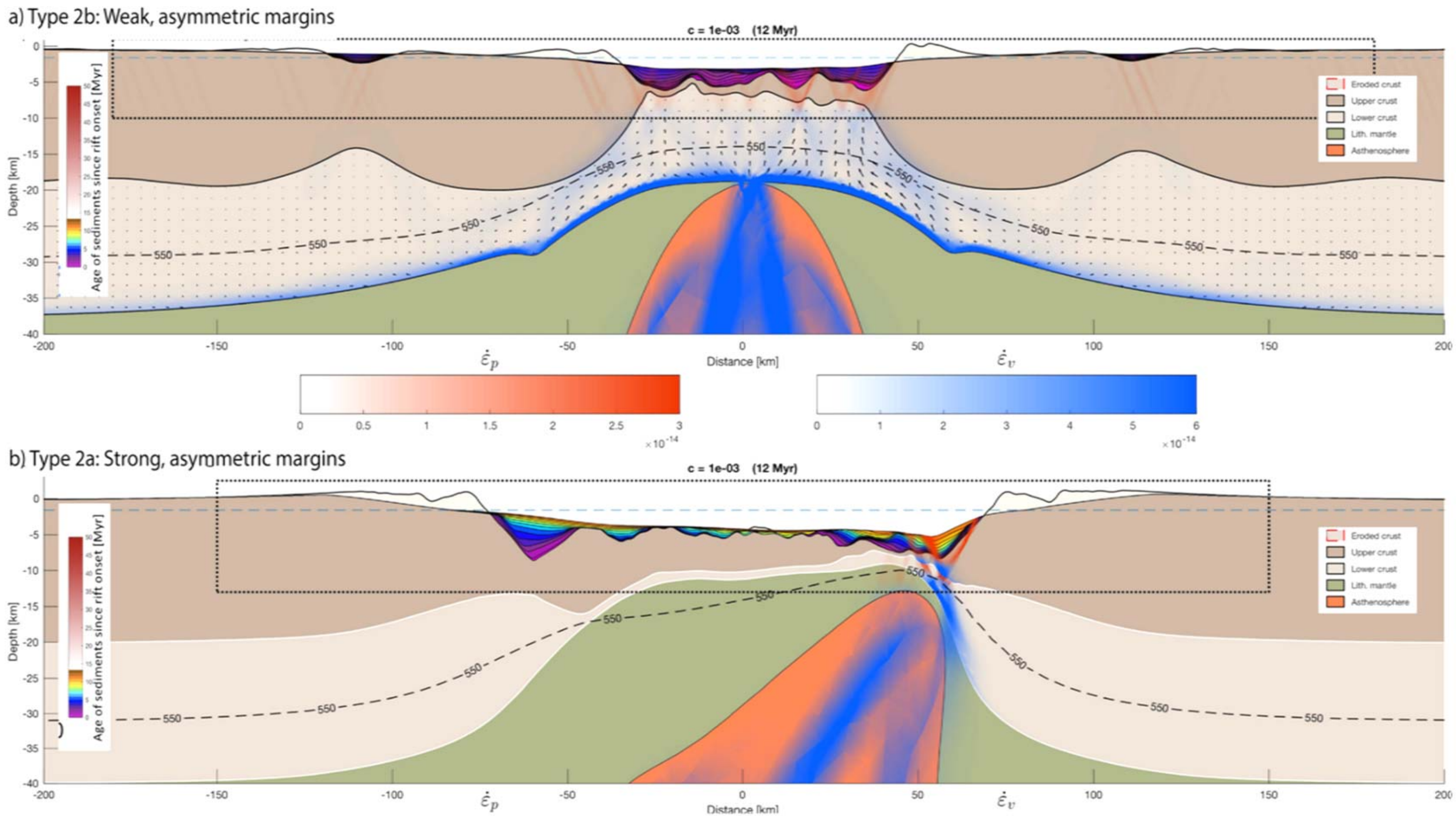

a) Type 2b: Weak, asymmetric margins
c = 1e-03 (12 Myr)
Depth [km]
Age of sediments since rift onset [Myr]
Eroded crust
Upper crust
Lower crust
Lith. mantle
Asthenosphere
550
Distance [km]
$\dot{\varepsilon}_p$
$\dot{\varepsilon}_v$
$\times 10^{-14}$
b) Type 2a: Strong, asymmetric margins
c = 1e-03 (12 Myr)

Figure S10. a) Type 2b and b) Type 2a models, at 12 Myr after rift start. Dashed black line is the 550° C isotherm. Dashed blue line is sea-level. Red and blue shadings are plastic and ductile strain rate. Synrift sediments are shown in rainbow color. Comparison between the two figures shows that even if the lithospheric mantle has broken up at 12 million years in the weak model, i.e. Type 2b (a), the asthenosphere as well as the 550° C isotherm is deeper in the weaker, (a), than in the stronger model (b), where the lithospheric mantle has not yet broken up. Thus, the model in (a) does not have a higher geothermal gradient than the model in (b). The less subsidence in the weaker model is thus not related to higher geothermal gradient due to early mantle lithosphere break-up, but to the existence of a very weak, thick lower crust which is translated in less crustal thinning and a shallower depth of necking in the weak model, (a), with respect to the strong one, (b). Black arrows in a) show the relative movement of lower with respect to upper crust, indicating that lower crust is flowing into the area of upper crustal deformation.

Table S1. Model parameters and rheological constants used for the numerical models presented in this work.

	Wet quartzite[1]	**Wet anorthite**[2]	**Mafic granulite**[3]	**Dry olivine**[4]	**Wet olivine**[5]
Thermomechanical parameters	(UC and weak LC)	(intermediate strength LC)	(strong LC)	(lithospheric mantle)	(asthenospheric mantle)
Dislocation pre-exponential factor $log(B_{dis})$ $[\mathrm{Pa^{-n}\ s^{-1}}]$	−28.0	−15.40	−21.05	−15.96	−15.81
Dislocation exponent n_{dis}	4.0	3.0	4.2	3.5	3.5
Dislocation activation energy E^*_{dis} $[\mathrm{kJ\ mol^{-1}}]$	223	356	445	530	480
Dislocation activation volume V^*_{dis} $[10^{-6}\ \mathrm{m^3\ mol^{-1}}]$	0	0	0	13	10
Diffusion pre-exponential factor $log(B_{dif})$ $[\mathrm{Pa^{-n}\ s^{-1}}]$	-	-	-	−8.16	−8.64
Diffusion exponent n_{dif}	-	-	-	1	1
Diffusion activation energy E^*_{dif} $[\mathrm{kJ\ mol^{-1}}]$	-	-	-	375	335
Diffusion activation volume V^*_{dif} $[10^{-6}\ \mathrm{m^3\ mol^{-1}}]$	-	-	-	6	4
	UC	LC	Lithospheric mantle	Asthenospheric mantle	
Shear modulus μ [GPa]	36	40	74	74	
Thermal conductivity k $[\mathrm{W\ m^{-1}\ K^{-1}}]$	2.1	2.5	3.3	3.3	
Heat capacity C_p $[\mathrm{J\ kg^{-1}\ K^{-1}}]$	1,200	1,200	1,200	1,200	
Radiogenic heat production H_r $[\mathrm{\mu W\ m^{-3}}]$	1.3	0.2	0	0	
Reference densities ρ_0 $[\mathrm{kg\ m^{-3}}]$	2,700	2,850	3,300	3,300	
Thermal expansivity coefficient α_T $[10^{-5}\ \mathrm{K^{-1}}]$	2.4	2.4	3.0	3.0	
Surface processes parameters		Value			
Surface processes time step δt_s [Kyr]		1			
Subaerial hillslope diffusion K $[\mathrm{m^2\ year^{-1}}]$ [7]		0.25			
Subaerial discharge transport coefficient c[8]		10^{-3}			
Pelagic sedimentation rate pe $[\mathrm{m^2\ year^{-1}}]$[9]	Syn-rift	$10^{-4}, 3\times10^{-4}$			
	Post-rift	1×10^{-5}			
Precipitation rate α $[\mathrm{m\ year^{-1}}]$ [10]		1			
Submarine diffusion coefficient K_s $[\mathrm{m^2\ year^{-1}}]$[11]		10^2			
Submarine diffusion coefficient decay λ_s $[\mathrm{m^{-1}}]$ [12]		10^{-3}			

Note. The remaining parameters are from Turcotte and Schubert (2002). Diffusion creep B is calculated using a grain size of 6 mm. Wet olivine water content is 500 ppm H/Si.

[a]Rheological parameters for upper crust (UC), lower crust (LC), lithospheric mantle, and asthenospheric mantle are from Gleason and Tullis (1995), Hirth and Kohlstedt (2003), and Wilks and Carter (1990). [b]Depletion factor for density dependence β is from Schutt and Lesher (2006). [c]Subaerial hillslope diffusion K is from Armitage et al. (2015). [d]Subaerial discharge transport coefficient c. [e]Pelagic

sedimentation rate pe is from Armitage et al. (2014), Marr et al. (2000), and Paola et al. (1992). [f]Precipitation rate α is from Huffman et al. (2009). [g]Submarine diffusion coefficient K_S. [h]Submarine diffusion coefficient decay λ_S is from Kaufman et al. (1991).

Repeat for any additional Supporting data sets

Movie S1. Shows evolution of Type 1a model: narrow, strong, symmetric margins (see Table 1, Figures 1a and 2). Top panel shows a general view of the model. Middle panel shows a zoom of the model. The upper, lower crust, mantle lithosphere and asthenosphere are color coded. Light brown: upper crust, beige: lower crust, green: lithospheric mantle, orange: asthenosphere. The red and blue shaded areas indicate the areas of highest plastic and ductile strain rate. The age of the sediments is color coded: rainbow scale shows sediments of synrift age, white to red scale shows sediments of postrift age. Dashed blue lines are sea-level. Dashed black lines are isotherms. Black lines with white background are $10^{20.5}$ Pa.s isoviscosity line. Bottom panel shows the depth trajectory of the markers shown in the above panels with time during model evolution. Blue vertical line marks the time step shown in the top panels.

Movie S2. Shows evolution of Type 1b model: narrow, weak, symmetric margins and lowest sedimentation rate shown here (Table 1). This movie corresponds to the evolution in Figure A7 (bottom). Top panel shows a general view of the model. Middle panel shows a zoom of the model. The upper, lower crust, mantle lithosphere and asthenosphere are color coded. Light brown: upper crust, beige: lower crust, green: lithospheric mantle, orange: asthenosphere. The red and blue shaded areas indicate the areas of highest plastic and ductile strain rate. The age of the sediments is color coded: rainbow scale shows sediments of synrift age, white to red scale shows sediments of postrift age. Dashed blue lines are sea-level. Dashed black lines are isotherms. Black lines with white background are $10^{20.5}$ Pa.s isoviscosity line. The eroded area is shown by a red line. SL: sea-level, and the thin black lines are only shown to highlight the uplift and subsidence of the blocks as the deformation migrates onceanward.

Movie S3. Shows evolution of Type 2a model: strong, asymmetric margins, and the highest sedimentation rate shown here (Table 1, Figures 1b and 4b). Top panel shows a general view of the model. Arrows show the differential flow of the lower crust with respect to upper crust. Middle panel shows a zoom of the model. The upper, lower crust, mantle lithosphere and asthenosphere are color coded. Light brown: upper crust, beige: lower crust, green: lithospheric mantle, orange: asthenosphere. The red and blue shaded areas indicate the areas of highest plastic and ductile strain rate. The age of the sediments is color coded: rainbow scale shows sediments of synrift age, white to red scale shows sediments of postrift age. Dashed blue lines are sea-level. Dashed black lines are isotherms. Black lines with white background are $10^{20.5}$ Pa.s isoviscosity line. Bottom panel shows the depth trajectory of the markers shown in the above panels with time during model evolution. Blue vertical line marks the time step shown in the top panels.

Movie S4. Shows evolution of Type 2b model: weak, asymmetric margins (Table 1, Figures 1c and 6). Top panel shows a general view of the model. Arrows show the differential flow of the lower crust with respect to upper crust. Middle panel shows a zoom of the model. The upper, lower crust, mantle lithosphere and asthenosphere are color coded. Light brown: upper crust, beige: lower crust, green: lithospheric mantle, orange: asthenosphere. Middle panel shows a zoom of the model. The red and blue shaded areas indicate the areas of highest plastic and ductile strain rate. The age of the sediments is color coded: rainbow scale shows sediments of synrift age, white to red scale shows sediments of postrift age. Dashed blue lines are sea-level. Dashed black lines are isotherms. Black lines with white background are $10^{20.5}$ Pa.s isoviscosity line. Bottom panel shows the depth trajectory of the markers shown in the above panels with time during model evolution. Blue vertical line marks the time step shown in the top panels.

Movie S5. Shows the same as in Movie 4, i.e. the evolution of Type 2b model: weak, asymmetric margins (Table 1, Figures 1c and 6) but the bottom panel shows the trajectory of different markers to those shown in Movie 4. Top panel shows a general view of the model. Middle panel shows a zoom of the model. The upper, lower crust, mantle lithosphere and asthenosphere are color coded. Light brown: upper crust, beige: lower crust, green: lithospheric mantle, orange: asthenosphere. Middle panel shows a zoom of the model. The red and blue shaded areas indicate the areas of highest plastic and ductile strain rate. The age of the sediments is color coded: rainbow scale shows sediments of synrift age, white to red scale shows sediments of postrift age. Dashed blue lines are sea-level. Dashed black lines are isotherms. Black lines with white background are $10^{20.5}$ Pa.s isoviscosity line. Bottom panel shows the depth trajectory of the markers shown in the above panels with time during model evolution. Blue vertical line marks the time step shown in the top panels.

Movie S6. Shows evolution of Type 3 model: wide, symmetric margins (Table1, Figures 1d, 8, 9, 16 A2d, A6c). Top panel shows a general view of the model. Middle panel shows a zoom of the model. The upper, lower crust, mantle lithosphere and asthenosphere are color coded. Light brown: upper crust, beige: lower crust, green: lithospheric mantle, orange: asthenosphere. Middle panel shows a zoom of the model. The red and blue shaded areas indicate the areas of highest plastic and ductile strain rate. The age of the sediments is color coded: rainbow scale shows sediments of synrift age, white shows sediments of postrift age. Dashed blue lines are sea-level. Dashed black lines are isotherms. Black lines with white background are $10^{20.5}$ Pa.s isoviscosity line. Bottom panel shows the depth trajectory of the markers shown in the above panels with time during model evolution. Blue vertical line marks the time step shown in the top panels.

Movie S7. Viscosity evolution for the 4 main models discussed in Figure 1a. Thin black line on top of thicker white line is the base of the continental lithosphere. Dashed black lines are isotherms and white lines are isoviscosity lines in MPa.

Movie S8. Horizontal stress evolution, in MPa, for the 4 main models discussed in Figure 1. Black arrows show the differential flow of the lower crust with respect to upper crust. Black line on top of white line is base of continental lithosphere. Dashed black lines are isotherms and blue lines are isoviscosity lines in MPa. Strain rate is shown in grey shades.

Movie S9. Shows evolution of Type 2c model: intermediate strength, asymmetric margins (Table1, Figure 13). Top panel shows a general view of the model. Bottom panel shows a zoom of the model. The upper, lower crust, mantle lithosphere and asthenosphere are color coded. Light brown: upper crust, beige: lower crust, green: lithospheric mantle, orange: asthenosphere. The red and blue shaded areas indicate the areas of highest plastic and ductile strain rate. The age of the sediments is color coded: rainbow scale shows sediments of synrift age, white to red scale shows sediments of postrift age. Dashed blue lines are sea-level. Dashed black lines are isotherms. Black lines with white background are the $10^{20.5}$ Pa.s isoviscosity lines.